J. Opt. **12** (2010) 075703 (8pp) doi:10.1088/2040-8978/12/7/075703

Wavelength modulated optical reflectivity spectra of $CuAl_{1-X}Ga_XSe_2$ crystals

N N Syrbu[1], A V Dorogan[1], V V Ursaki[2] and A Masnik[1]

[1] Technical University of Moldova, Stefan cel Mare Street 168, Chisinau, MD-2004, Moldova
[2] Institute of Applied Physics, Academy of Sciences of Moldova, Academy Street 5, Chisinau, MD-2028, Moldova

Received 31 March 2010, accepted for publication 1 June 2010
Published 1 July 2010
Online at stacks.iop.org/JOpt/12/075703

Abstract
Exciton spectra of $CuAl_{1-X}Ga_XSe_2$ solid solutions are investigated by wavelength modulated optical reflectivity at low temperatures (10 K). The energy position of $n = 1$ and 2 lines of the $\Gamma_4(A)$, $\Gamma_5(B)$ and $\Gamma_5(C)$ exciton series, as well as the $\Gamma_7(V_1)$–$\Gamma_6(C_1)$, $\Gamma_6(V_2)$–$\Gamma_6(C_1)$, $\Gamma_7(V_3)$–$\Gamma_6(C_1)$ energy intervals, and the crystal field and spin–orbit splitting of the valence band are determined. The effective electron mass (m^*_{C1}) and hole masses (m^*_{V1}, m^*_{V2}, m^*_{V3}) are estimated for $CuAl_{1-X}Ga_XSe_2$ solid solutions as a function of the X value.

Keywords: reflection spectra in semiconductors, optical constants, excitons and polaritons

1. Introduction

$CuGaSe_2$ and $CuAlSe_2$ compounds, as well as their solid solutions belonging to the I–III–VI_2 materials crystallize in the chalcopyrite structure with the $I42d$–D^{12}_{2d} space group. Stimulated emission and second harmonic generation at 10.6 μm as well as generation of infrared (IR) radiation in the region of 4.6 and 12 μm was realized in these compounds [1–4]. Biexcitons [5], interference of additional waves [6], resonance Raman scattering [7–9] and intense emission due to exciton polaritons and bound excitons [10–12] have been observed in these crystals. Optoelectronic devices and solar cells are developed on the basis of these materials [13–19]. The photoluminescence properties of $CuAlSe_2$ crystals doped with Er^{3+} ions [15] as well as the photoelectrical properties of surface barrier structures on the basis of $CuAlSe_2$ have been studied [17, 18]. These materials possess a strong anisotropy of optical properties in the visible and infrared spectral ranges which is very important for the development of polarized optoelectronic devices.

The goal of this paper is to investigate the main exciton parameters as well as the energy gaps at the center of the Brillouin zone as a function of composition of $CuAl_{1-X}Ga_XSe_2$ solid solutions. The energy position of $n = 1$ and 2 lines of the $\Gamma_4(A)$, $\Gamma_5(B)$ and $\Gamma_5(C)$ exciton series, as well as the $\Gamma_7(V_1)$–$\Gamma_6(C_1)$, $\Gamma_6(V_2)$–$\Gamma_6(C_1)$, $\Gamma_7(V_3)$–$\Gamma_6(C_1)$ energy intervals, are determined from wavelength modulated optical reflectivity spectra. The effective electron mass (m^*_{C1}), and hole masses (m^*_{V1}, m^*_{V2}, m^*_{V3}), are estimated from the analysis of exciton reflectivity spectra according to a single-oscillator model of dispersion relations. The asymmetry parameters of reflectivity spectra are determined.

2. Experimental details

$CuAl_{1-X}Ga_XSe_2$ crystals in the form of platelets with 2.5 × 1.0 cm^2 mirror-like surfaces and thicknesses of 300–400 μm were grown by chemical vapor transport [16]. The surface plane of the platelets contains the C-axis. The optical reflectivity and wavelength modulated spectra were measured using a MDR-2 (LOMO, Russia) spectrometer. For low-temperature measurements, the samples were mounted on the cold station of a LTS-22 C 330 optical cryogenic system.

3. Results and discussions

According to theoretical calculation of the band structure of $CuAl_{1-X}Ga_XSe_2$ crystals with $I42d$–D^{12}_{2d} space group [20, 21], the minimum energy gap is formed by direct electron transitions at the center of the Brillouin zone. The lower conduction band has a Γ_6 symmetry, while the upper V_1, V_2, and V_3 valence bands are of Γ_7, Γ_6, and Γ_7 symmetry, respectively.

The interaction of electrons from the conduction band Γ_6 and holes from the valence band Γ_7 is determined by the product of irreducible representations $\Gamma_1 \times \Gamma_6 \times \Gamma_7 = \Gamma_3 + \Gamma_4 + \Gamma_5$ [21, 22]. The $\Gamma_4(A)$ exciton allowed in $E \parallel c$ polarization, Γ_5 exciton allowed in $E \perp c$ polarization

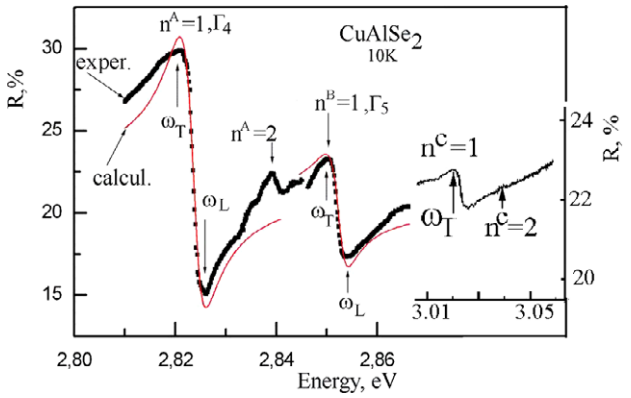

Figure 1. Reflectivity spectra for the $\Gamma_4(A)$, $\Gamma_5(B)$, and $\Gamma_5(C)$ excitons in $CuAlSe_2$ crystals measured at $T = 10$ K.

(This figure is in colour only in the electronic version)

and Γ_3 exciton forbidden in both polarizations are formed as a result of this interaction. In the short-wavelength region, the $\Gamma_1 \times \Gamma_6 \times \Gamma_6 = \Gamma_1 + \Gamma_2 + \Gamma_5$ interaction leads to the formation of the Γ_5 exciton series (B-exciton series) which is allowed in the $E \perp c$ polarization, and Γ_1 and Γ_2 excitons which are forbidden in both polarizations. Three exciton series Γ_1, Γ_2 and Γ_5 are produced as a result of interaction of electrons from the C_1 conduction band with holes from the V_2 valence band with Γ_6 symmetry. The $\Gamma_5(B)$ excitons are allowed and the Γ_1 and Γ_2 excitons are forbidden in the $E \perp c$ polarization according to selection rules. The interaction of electrons from the C_1 conduction of the Γ_7 symmetry with holes from the V_3 valence band with Γ_7 symmetry leads to the formation of Γ_3, Γ_4 and Γ_5 excitons. The Γ_3 excitons are forbidden, the $\Gamma_5(C)$ exciton is allowed, and the Γ_4 exciton is partially allowed in the $E \perp c$ polarization. In this case, the Γ_4 exciton has a lower oscillator strength as compared to the Γ_5 exciton.

The $n = 1$ ($\omega_t = 2.8212$ eV, $\omega_L = 2.8237$ eV) and $n = 2$ (2.8390 eV) lines as well as a weak line at 2.8442 eV corresponding to the $n = 3$ state of the $\Gamma_4(A)$ exciton hydrogen-like series are observed in the reflectivity spectra of $CuAlSe_2$ crystals measured at 10 K in the $E \parallel c$, $\kappa \perp c$ polarization (figure 1).

The reflectivity spectra in the region of the $n = 1$ line of the $\Gamma_4(A)$ exciton are of a usual excitonic shape with a maximum at 2.8212 eV and a minimum at 2.8237 eV. These peculiarities are due to the presence of the transverse and longitudinal excitons. A longitudinal–transverse exciton splitting of 2.5 meV is estimated for the Γ_4 excitons from these data. A Rydberg constant of 24 meV is determined for the Γ_4 exciton series from the position of $n = 1$ and 2 lines (figure 1). The energy of the continuum (E_g, $n = \infty$) is equal to 2.845 eV. The energy position of the ground ($n = 1$) states of $\Gamma_4(A)$, $\Gamma_5(B)$, and $\Gamma_5(C)$ excitons have been previously determined to be 2.737, 2.851 and 3.012 eV, respectively, in $CuAlSe_2$ crystals at 77 K [23, 24]. The contours of reflectivity spectra have not been analyzed in these papers, and the translation and reduced exciton masses have not been calculated. A mean value of the ground exciton state energy E_{ex} has been determined from the wavelength modulated spectra, which is lower than the energy of the longitudinal exciton, and is higher than the energy of the transverse exciton.

The reflection coefficient and the background dielectric constant in the region of exciton resonances are equal to 0.24–0.25, and 7.4–8.2, respectively, varying from sample to sample. A reflection coefficient value of 0.25 has been reported for $CuAlSe_2$ crystals at 300 K [25]. The value of the background dielectric constant determined from optical spectra in the infrared region is lower [26–28]. The value of the background dielectric constant determined from the reflectivity spectra near the exciton resonances has been used in our calculations. The reflection coefficient in the $E \parallel c$ polarization at 10 K equals 0.25, which corresponds to a background dielectric constant of 7.6. With $\varepsilon_b = 7.6$ and Rydberg constant $R = 0.024$ eV, the Γ_4-excitons reduced mass equals $\mu = \varepsilon_b^2 R/R_H = 0.1m_0$, where R_H is the Rydberg energy of the hydrogen atom (13.6 eV). The Bohr radius (a_B) of the S-state of the $\Gamma_4(A)$-exciton equals 0.21×10^{-6} cm.

A maximum at 2.851 eV (transverse exciton) and a minimum at 2.853 eV (longitudinal exciton) are observed in the $E \perp c$ polarization for the $\Gamma_5(B)$ exciton series (figure 1). The longitudinal–transverse splitting of the $\Gamma_5(B)$ exciton equals 2.0 meV. The $n = 2$ excited exciton state is observed at 2.868 eV. The binding energy of the Γ_5 exciton is determined to be 22 meV, and the energy of the continuum is equal to 2.873 eV.

The calculations of the reflectivity spectra are usually carried out within the framework of classical optics taking into account the spatial dispersion and the presence of a dead layer [29–33]. The damping parameter γ is small in high quality crystals. If $\omega_{LT} \gg \gamma$ and $M \neq \infty$, one can consider that there is a strong exciton–photon interaction (strong polariton effect). In this case, the translation exciton mass, the energy of longitudinal and transverse excitons, the damping parameter, and the presence or the absence of an exciton dead layer on the crystal surface can be determined from the calculations of reflectivity spectra. The movement of elementary electron excitations in a crystal is characterized by the transport of kinetic energy $\hbar k^2/2M$, where $P = \hbar k$ is the exciton quasi-momentum, and $M = m_e^* + m_h^*$ [30, 31]. One needs in many cases to take into account the dependence of the translation mass on the direction of the wavevector with respect to crystal axes (the phenomenon of anisotropy). The excitation is localized when $M \to \infty$, and the spatial dispersion is practically absent in this case. On the contrary, there is a weak polariton effect when the longitudinal–transverse splitting is small and $\omega_{LT} \ll \gamma$.

The dielectric function in the region of exciton resonance is written as

$$\varepsilon(\omega, k) = \varepsilon_b + \frac{2\varepsilon_b \omega_{LT} \omega_0}{\omega_0 - \omega + \frac{\hbar^2 k^2}{2M}\omega_0 - i\gamma\omega}. \qquad (1)$$

The reflectivity from an isotropic crystal in the case of normal incident light is determined by

$$R = \left| \frac{\left(\frac{1-n_0}{1+n_0}\right) + \left(\frac{n_0-n^*}{n_0+n^*}\right) e^{i2kn_0 t}}{1 + \left(\frac{1-n_0}{1+n_0}\right)\left(\frac{n_0-n^*}{n_0+n^*}\right) e^{i2kn_0 t}} \right|^2 \qquad (2)$$

where $n_0 = \sqrt{\varepsilon_b}$, $n^* = \frac{n_1 n_2 + \varepsilon_0}{n_1 + n_2}$, ε_b is the background dielectric constant, t is the dead layer thickness, k is the exciton wavevector, and n_1 and n_2 are longitudinal and transverse components of the refractive index determined from

$$n_{1,2}^2 = \frac{1}{2}\left\{\left(\varepsilon_b + \frac{2Mc^2(\omega-\omega_0)}{\hbar\omega_0^2}\right) \pm \left[\left(\frac{2Mc^2(\omega-\omega_0)}{\hbar\omega_0^2} - \varepsilon_b\right)^2 + \frac{8Mc^2\varepsilon_b\omega_{LT}}{\hbar\omega_0^2}\right]^{1/2}\right\}. \quad (3)$$

A comparison of the calculated and the measured contours of the reflectivity spectra for the ground state of the Γ_4(A) and Γ_5(B) excitons is presented in figure 1. A best fit of experimental data for the Γ_4(A) exciton is obtained with the following parameters: $\varepsilon_b = 7.6 \pm 0.2$, $\omega_T = 2.8220 \pm 0.0010$ eV, $\omega_{LT} = 2.5 \pm 0.2$ meV, $\gamma = 3.5 \pm 0.3$ meV, $t = 0$.

The translation mass M of the Γ_4(A) excitons determined from these calculations for the $CuAlSe_2$ crystals equals $(1.2 \pm 0.1)m_0$, while for the Γ_5(B) excitons a translation mass of $(0.5–0.8)m_0$ is determined. The C exciton is also observed in this polarization at the energy of 3.023 eV ($n = 1$) and 3.039 eV ($n = 2$). The Rydberg constant equals 21 meV, and the energy gap of 3.044 eV is estimated for the C excitons.

The effective masses in the conduction and the valence bands have been determined on the basis of these data, and taking into account that $M = m_V^* + m_C^*$ and $1/\mu = 1/m_V^* + 1/m_C^*$, where m_C^*, m_V^* are the effective masses in the conduction band and in the $\Gamma_7(V_1)$, $\Gamma_6(V_2)$, $\Gamma_7(V_3)$ valence bands. With $M = 1.3m_0$ and $\mu = 0.10m_0$, one obtains the electron effective mass $m_C^* = 0.11m_0$, and the effective mass of holes $m_{V1}^* = 1.20m_0$. Nearly the same values of m_C^* and m_{V1}^* are obtained with $M = 1.1m_0$. The errors in the range of $0.2m_0$ in the determination of the M value from the reflectivity spectra do not significantly influence the obtained values of m_C^* and m_{V1}^*.

The obtained values of m_C^* and m_{V1}^* for the $CuAlSe_2$ are very close to those obtained previously for the $CuGaSe_2$ crystals [34]. The parameters of the Γ_5(B) excitons differ insignificantly from those of the Γ_4(A) excitons. The effective mass of electrons equal to 0. $11m_0$, and hole masses $m_{V2}^* = (0.4–0.7)m_0$ are obtained for the Γ_5(B)-excitons with the translation mass $M = (0.5–0.8)m_0$ and the Rydberg constant $R = 21$ meV. Unfortunately, we were not able to determine the value of m_{V2}^* with better accuracy. For the C-exciton series the reduced effective mass $\mu = 0.076m_0$ and the effective mass of holes $m_{V3}^* = 0.25m_0$ are obtained (table 2). One should note that the contour of reflectivity spectra was not calculated for the Γ_5(C) exciton, since the quality of the experimental spectrum is not enough for this purpose. Instead, the value of m_{V3}^* was determined from the relation $1/\mu = 1/m_v^* + 1/m_c^*$. We assume that the electron mass in these crystals is practically identical for the Γ_4(A), Γ_5(B), and Γ_5(C) excitons, while the value of the reduced mass μ was determined experimentally. One should also note that these calculations only allow one to determine the effective carrier masses, not to assign them to the conduction or valence band. The assignment is done by comparing the effective masses found from different exciton bands assuming that the electron effective mass should be the same for all exciton bands as mentioned above, and taking into account that usually the electron mass is smaller than the hole mass. Apart from that, data available for other materials are taken into account such as $CuGaSe_2$ [34, 35], $CuInSe_2$ [36], $CuInTe_2$ [37], and $CuGaS_2$ [38–41] crystals.

The reflectivity spectra of $CuGaSe_2$ crystals have been discussed previously [34, 39]. The $n = 1$ line ($\omega_t = 1.7380$ eV, $\omega_L = 1.7405$ eV) and the $n = 2$ line (1.7650 eV) of the Γ_4(A) excitons are revealed in these spectra measured at the temperature of 10 K in the $E \parallel c, \kappa \perp c$ polarization [34]. A longitudinal–transverse exciton splitting of 2.5 meV, a Rydberg constant of 36 meV, and the energy of the continuum (E_g, $n = \infty$) equal to 1.7738 eV, are estimated for the Γ_4 excitons from these data.

A maximum at 1.8215 eV (transverse exciton) and a minimum at 1.8235 eV (longitudinal exciton) are observed in the $E \perp c$ polarization for the Γ_5(B) exciton series [34]. The longitudinal–transverse splitting equals 2.0 meV for the Γ_5(B) exciton. The $n = 2$ excited state is observed at 1.8483 eV. The Rydberg constant is equal to 35.5 meV, and the energy of the continuum is 1.8575 eV for the Γ_5(B) exciton. The Γ_5(C) exciton is revealed in the same polarization at 2.023 eV ($n = 1$) and 2.038 eV ($n = 2$). The coincidence of the calculated and the measured reflectivity contours has also been discussed [34, 38, 39]. In $CuGaSe_2$ crystals the exciton translation mass is equal to $1.4m_0$ for the Γ_4(A) and Γ_5(B) excitons, and $1.0m_0$ for the Γ_5(C) excitons (table 2). The spectral dependence of the refractive index and the coefficient of absorption has also been determined from the calculations of the exciton reflectivity spectra [34]. The main exciton parameters and the energy gaps are summarized in tables 1 and 2 [34]. The electron mass $m_C^* = 0.14m_0$, and the hole mass $m_{V1}^* = 1.26m_0$ have been deduced for these crystals with the values of $M = 1.4m_0$ and $\mu = 0.13m_0$. The obtained value of $m_{V1}^* = 1.26m_0$ coincides in the limits of experimental errors with the previously reported one of $1.2m_0$ [34]. Taking into account that the parameters of the Γ_5(B) excitons insignificantly differ from those of the Γ_4(A) excitons, the m_{V2}^* effective mass is also equal to $1.26m_0$ [34], i.e. it practically coincides the m_{V1}^* value.

The wavelength modulated reflectivity spectra of $CuAlSe_2$ and $CuGaSe_2$ crystals are presented in figures 2 and 3, respectively. The $n = 1$ and 2 lines of the Γ_4(A), Γ_5(B) and Γ_5(C) excitons are revealed in the spectra for both the compositions. Apart from that, the $n = 3$ line of the Γ_4(A) exciton is observed in the spectrum of the $CuAlSe_2$ crystals. Two states of the Γ_4(A) exciton series in $CuGaSe_2$ crystals are observed at 1.740 eV ($n = 1$) and 1.766 eV ($n = 2$), while the Γ_5(B) exciton series is observed at 1.822 eV ($n = 1$) and 1.848 eV ($n = 2$). Additionally, the s-state of the Γ_5(C) excitons is observed at 2.030 eV. As expected, the maximum of the first derivative of reflectivity spectrum for exciton states corresponds to an intermediate energy between the energy of the longitudinal and transversal exciton. The relative increment of the reflection coefficient $\Delta R/R$ is measured in wavelength modulated spectra. At the same time, the expressions for the $\Delta\varepsilon_1$ and $\Delta\varepsilon_2$ increments of the real (ε_1) and imaginary (ε_2) components of the dielectric function ε are obtained from

Table 1. Parameters of exciton spectra in $CuAl_XGa_{1-X}Se_2$ crystals. (Note: Asterisks indicate values determined from the calculations of reflectivity contours.)

$CuAl_XGa_{1-X}Se_2$ composition	Exciton states	*A*-exciton energy (eV)	*B*-exciton energy (eV)	*C*-exciton energy (eV)
$X = 0.0$ ($CuGaSe_2$)	$n = 1$	1.7380 (1.7385*)	1.8235*	2.022
According to [34]	$n = 2$	1.7650	1.8483	
and this work	R	0.036	0.0357	
	E_g	1.7745	1.8592	
$X = 0.2$	$n = 1$	1.920*	1.980	2.200
	$n = 2$	1.943	2.002	2.218
	R	0.030	0.029	0.024
	E_g	1.950	2.009	2.224
$X = 0.3$	$n = 1$	1.980	2.08	2.280
	$n = 2$	2.000	—	—
	R	0.027	—	—
	E_g	2.007	—	—
$X = 0.4$	$n = 1$	2.080	2.190	2.400
	$n = 2$	2.102	2.211	2.418
	R	0.029	0.028	0.024
	E_g	2.209	2.218	2.424
$X = 0.5$	$n = 1$	2.180*	2.280	2.500
	$n = 2$	2.202	2.299	2.518
	R	0.029	0.027	0.024
	E_g	2.209	2.307	2.524
$X = 0.7$	$n = 1$	2.480	2.522	2.680
	$n = 2$	2.500	2.540	2.697
	R	0.026	0.024	0.023
	E_g	2.506	2.546	2.703
$X = 0.8$	$n = 1$	2.483 (2.482*)	2.575	2.770
	$n = 2$	2.501	2.592	2.786
	R	0.024	0.023	0.021
	E_g	2.507	2.598	2.791
$X = 1.0$	$n = 1$	2.8212 (2.8220*)	2.851(2.8520*)	3.023
$CuAlSe_2$	$n = 2$	2.8390	2.868	3.039
	$n = 3$	2.8442	—	—
	R	0.024	0.022	0.018
	E_g	2.8450	2.873	3.044

Table 2. Dielectric constants, exciton parameters and bandgaps in $CuAl_{1-X}Ga_XSe_2$ crystals.

X	1.0 [34]	0.8	0.5	0.2	0.0
$\varepsilon^{\parallel}/\varepsilon^{\perp}$	4.2/5.1	4.9/5.5	5.8/6.0	6.3/6.9	6.67/8.28
ε_b	7.0	7.2	7.3	7.4	7.4–8.2
μ^A	$0.13m_0$	0.12	0.13	0.11	$0.11m_0$
μ^B	$0.13m_0$	0.12	0.11	0.11	$0.099m_0$
μ^C		0.097	0.09	0.08	$0.07m_0$
M^A_{exc}	$1.4m_0$	$1.3m_0$	$1.2m_0$	$1.1m_0$	$(1.1–1.3)m_0$
m_C	$0.14m_0$	$0.13m_0$	$0.12m_0$	$0.12m_0$	$0.11m_0$
m_{V1}	$1.26m_0$	$1.24m_0$	$1.23m_0$	$1.20m_0$	$1.20m_0$
m_{V2}	$1.26m_0$				$(0.4–0.7)m_0$
m_{V3}					$0.25m_0$

theoretical considerations. The expression for the $\Delta R/R$ as a function of $\Delta\varepsilon_1$ and $\Delta\varepsilon_2$ can be written as [42]

$$\Delta R/R = \alpha(\varepsilon_1, \varepsilon_2)\Delta\varepsilon_1 + \beta(\varepsilon_1, \varepsilon_2)\Delta\varepsilon_2, \qquad (4)$$

where

$$\alpha = C_1[(\varepsilon_1 - 1)A_+ + \varepsilon_2 A_-],$$

$$\beta = C_2[(\varepsilon_1 - 1)A_+^{-1} - \varepsilon_2 A_-^{-1}],$$

$$A_\pm = \pm\frac{\sqrt{2}[(\varepsilon_1^2 + \varepsilon_2^2)^{1/2} \pm \varepsilon_1]^{1/2}}{(\varepsilon_1^2 + \varepsilon_2^2)^{1/2}},$$

$$C_1 = [(\varepsilon_1 - 1)^2 + \varepsilon_2^2]^{-1},$$

$$C_2 = 2\varepsilon_2/[(\varepsilon_1 - 1)^2 + \varepsilon_2^2](\varepsilon_1^2 + \varepsilon_2^2).$$

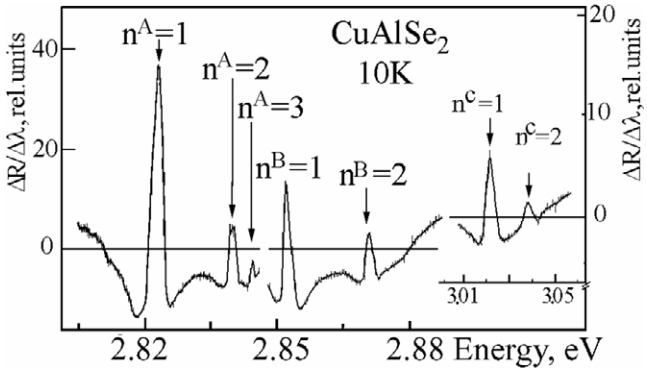

Figure 2. Wavelength modulated reflectivity spectra of $CuAlSe_2$ crystals measured at $T = 10$ K.

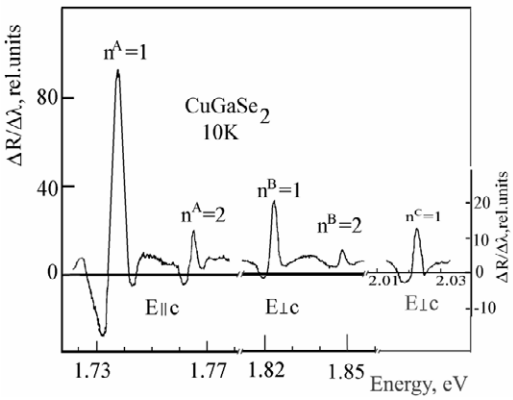

Figure 3. Wavelength modulated reflectivity spectra of $CuGaSe_2$ crystals measured at $T = 10$ K.

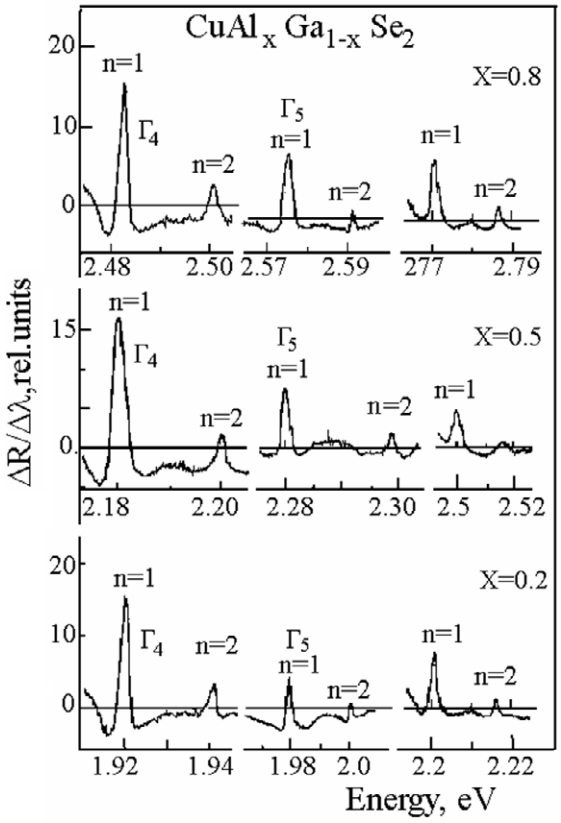

Figure 4. Wavelength modulated reflectivity spectra of $CuAl_{1-X}Ga_XSe_2$ crystals with $X = 0.8$, 0.5, and 0.2 measured at $T = 10$ K.

As one can see, $\Delta R/R$ depends on both $\Delta\varepsilon_1$ and $\Delta\varepsilon_2$. One of the α or β coefficients is much bigger than the other one in the region of the fundamental absorption edge. The contours of wavelength modulated reflectivity spectra for the $n = 1$ line of the Γ_4(A), Γ_5(B) and Γ_5(C) excitons have been calculated taking into account the spatial dispersion and the presence of a dead layer. The calculated spectra coincide better with the experimental ones when the dielectric constant has a small gradient. This gradient is determined by ε_b^{max} and ε_b^{min}. The minimum value of the background dielectric constant ε_b^{min} corresponds to the energy at which the exciton state starts to give input on the reflectivity spectrum, while the maximum value ε_b^{max} corresponds to the energy at which the s-state of the exciton does not influence anymore the reflectivity spectrum (there is no input on the ε). The gradient $\Delta\varepsilon$ is smaller than 0.15 for any of the exciton series. This gradient is due to the fact that there is an input on the dielectric constant from the B-exciton series in the frequency interval corresponding to the transitions in the s-state of the A excitons, which increases insignificantly with the increase of the frequency of the light.

Note that the wavelength modulated reflectivity spectra allow one a better determination of the ground and excited exciton states (figure 3). At the same time, such parameters as exciton masses, and frequencies of longitudinal (ω_L) and transversal (ω_T) excitons are determined with bigger errors as compared to the non-modulated reflectivity spectra. Therefore, we determined these parameters from the reflectivity spectra, not from the wavelength modulated ones. The structure of the wavelength modulated spectra (figure 4) was used for the determination of the Rydberg constant and the parameters of the energy bands (table 2). The structure of exciton lines is situated in the energy interval from 1.74 to 2.83 eV for all compositions of the investigated solid solutions. The $n = 1$ and 2 lines of the Γ_4(A), Γ_5(B) and Γ_5(C) excitons are observed in the wavelength modulated spectra of all solid solutions. The main exciton parameters and the energy gaps have been determined from the energy position of the $n = 1$ and 2 exciton lines (table 2).

The position of the $n = 1$ line demonstrates a nonlinear dependence on X in $CuAl_{1-x}Ga_XSe_2$ solutions (figure 5). The exciton binding energy (Rydberg constant) decreases linearly with the transition from $CuGaSe_2$ to $CuAlSe_2$ (table 1, figure 5). A weak deviation from linearity is observed for the energy gap, i.e. the energy interval Γ_7 (V_1)–Γ_6(C_1) (figure 5). The dependence of the energy intervals for the Γ_4(A), Γ_5(B) and Γ_5(C) excitons upon the composition is described by the polynomial

$$E_g(X) = E_g^1 X + E_g^2(1 - X) - CX(X - 1), \qquad (5)$$

where E_g^1 and E_g^2 are the bandgaps of the $CuGaSe_2$ and $CuAlSe_2$ compounds, respectively, and C is the coefficient

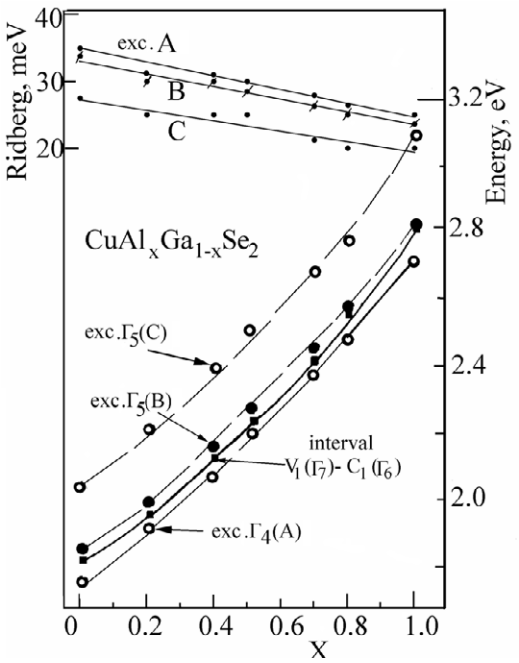

Figure 5. Dependence of the energy position of ground exciton states and binding energy of $\Gamma_4(A)$, Γ_5(B) and Γ_5(C) excitons upon the composition of solid solutions (X).

of nonlinearity. The deviation from linearity is weak (C equals 0.07–0.1) for the investigated solid solutions. A similar deviation from linearity is inherent to most of the I–III–VI_2 solid solutions. The C parameter equals 0.39 and 0.31 for the $CuGa(S_XSe_{1-X})_2$ and $CuIn_XGa_{1-X}S_2$ compounds, while it is around 0.29–0.34 for $CuAl_XGa_{1-X}S_2$ solutions. Therefore, the value of the C parameter is a little lower for the $CuAl_{1-X}Ga_XSe_2$ solid solutions.

In the following we will calculate the wavelength modulated reflectivity spectra for the case of weak polariton interaction. According to the theory of Hopfield and Toyozawa [42, 43], the absorption coefficient in the n exciton state at ω frequency is proportional to the asymmetrical Lorentz coefficient

$$\frac{\Gamma_n + 2A_n[\hbar\omega - (E_{ex,n} + \Delta_n)]}{[\hbar\omega - (E_{ex,n} + \Delta_n)]^2 + \Gamma_m^2}, \tag{6}$$

where Γ_n is the half width at full maximum resulting from the broadening of the n level due to the scattering on phonons. Δ_n is the input on the exciton energy $E_{ex,n}$ from the lattice vibrations. A_n is an asymmetry coefficient which differs from zero due to the weak dependence of the exciton density of states upon energy near the absorption peak.

The Γ_n and A_n parameters are considered to be independent of the $\hbar\omega$ photon energy in the interval $|\hbar\omega - E_{ex,n}| \leqslant \Gamma_n$ in the case of a weak exciton–phonon interaction. In the case of a strong exciton–phonon interaction, i.e. a high value of Γ_n, the contour of the line described by expression (6) will change due to the dependence of Γ and A values on ω in the interval $|\hbar\omega - E_{ex,n}| \approx \Gamma_n$, and will not demonstrate anymore an asymmetrical Lorentzian shape. The shape of each line will be Gaussian in the limit of strong interaction.

Hopfield suggested that the most probable mechanism determining the line shape is the scattering on optical phonons [43]. Toyozawa performed a more thorough analysis taking into account the transitions between different exciton states due to the exciton–phonon interaction (the consideration of the inter-band scattering) [42]. It was shown that the exciton absorption spectrum can be considered as a superposition of individual asymmetrical Lorentzian (6) absorption bands (the additive rule). The asymmetry coefficient is basically determined by the inter-band scattering [42]. By taking the derivative from the real and imaginary components of the dielectric function ε one can obtain the following expressions for the ε_1 and ε_2 derivatives:

$$\frac{\partial\varepsilon_1}{\partial\omega} = \frac{(\hbar\omega - E_{ex})^2 - \Gamma^2 - 4A\Gamma(\hbar\omega - E_{ex})}{[(\hbar\omega - E_{ex})^2 + \Gamma^2]^2} \tag{7}$$

$$\frac{\partial\varepsilon_2}{\partial\omega} = \frac{2A[\Gamma^2 - (\hbar\omega - E_{ex})^2] - 2\Gamma(\hbar\omega - E_{ex})}{[(\hbar\omega - E_{ex})^2 + \Gamma^2]^2}. \tag{8}$$

The main attention has been paid to the fitting of the central part of the excitonic band with the A and Γ parameters, taking into account the determining role of the LO phonons in the formation of this part of the excitonic band [42]. The reflectivity spectra change from minimum to maximum in this region of the spectrum. The A and Γ parameters are determined from the position of zeros and minima in the spectrum. One should mention that the theoretical curves are strongly influenced even by small changes of these parameters, which is evidenced by a comparison with the experimental curves.

The interaction of excitons with lattice vibrations leads to the broadening and the shift of exciton lines. It was shown [42] that the shape of the exciton line is Lorentzian in the case of a weak exciton–phonon interaction and a low value of the effective exciton mass, while it is Gaussian in the case of a strong exciton–phonon interaction and a high value of the effective exciton mass. For a weak or intermediate exciton–phonon interaction the exciton dispersion is expressed as

$$\varepsilon(\omega) \cong \frac{2A - 1}{(\hbar\omega - E_{exc})} - i\Gamma \tag{9}$$

where Γ is the half width at full maximum resulting from the broadening of the exciton level due to the scattering on phonons, E_{exc} is the exciton transition energy, and A is an asymmetry coefficient which differs from zero due to a weak dependence of the exciton density of states on energy near the absorption peak.

A comparison of the experimental and the calculated spectra of wavelength modulated reflectivity for the $n = 1$ line of Γ_4(A) and Γ_5(B) excitons in $CuGaSe_2$ and $CuAlSe_2$ crystals is presented in figure 6. The best fit is produced in the case of a classical Lorentz oscillator and the absence of spatial dispersion. The analysis of the reflectivity spectra in the considered crystals suggested that a weak polariton interaction is inherent to all of the solid solutions, i.e. the damping parameter is bigger than or equal to the longitudinal–transverse exciton splitting. One comes to the same conclusion from the analysis of reflectivity spectra according to the dispersion

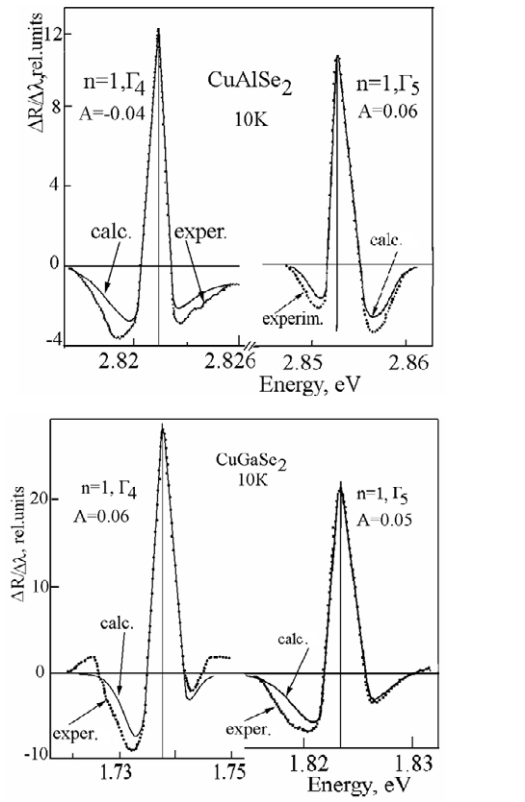

Figure 6. Experimental and calculated wavelength modulated reflectivity contours for the $n = 1$ state of Γ_4(A) and Γ_5(B) excitons in $CuAlSe_2$ and $CuGaSe_2$ crystals.

relations taking into account the spatial dispersion [34, 38, 39]. As one can see, the calculated spectra fit very well the experimental ones in the central part of the curves, while there is some difference at the wings. According to the Toyozawa theory, two types of oscillations contribute to the exciton band: one of which (LA or LO phonons) contributes to the central part and another one (TA phonons) contributes to the formation of wings [42]. Therefore, one can consider that the central part and the wings of the Γ_4(A), Γ_5(B), and Γ_5(C) bands are produced by different phonons. The shape of the Γ_4(A) and Γ_5(B) exciton lines at $T = 10$ K in $CuGaSe_2$ and $CuAlSe_2$ crystals is asymmetrical. The asymmetry factor A is equal to 0.06 and 0.04 for the Γ_4(C) excitons in $CuGaSe_2$ and $CuAlSe_2$ crystals, respectively. For the Γ_5(B) excitons, A equals 0.05 and 0.06 in $CuGaSe_2$ and $CuAlSe_2$ crystals, while it is around 0.01 for both compounds for the Γ_5(C) excitons (figure 7). This corresponds to the case of weak exciton–phonon interaction. One should mention that the damping parameter varies in the interval from 2.6 to 3.9 meV for the Γ_4(A), Γ_5(B), and Γ_5(C) excitons, while the longitudinal–transversal splitting does not exceed 3.4 meV [34]. The shape of the exciton lines becomes less asymmetrical, and the absolute value of the asymmetry coefficient does not increase with increasing temperature. This behavior of the shape of bands in the wavelength modulated reflectivity is due to the fact that the value of the damping parameter is higher than the longitudinal–transverse exciton splitting. The damping parameter for the Γ_4(A) excitons in solid solutions with $X =$

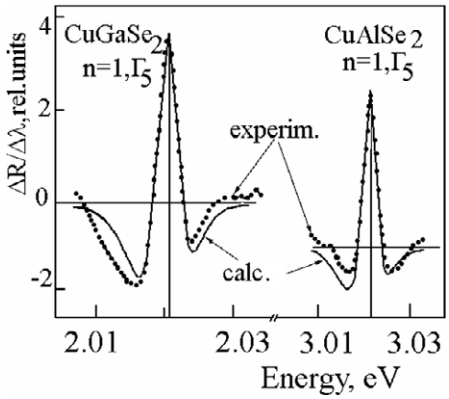

Figure 7. Experimental and calculated wavelength modulated reflectivity contours for the $n = 1$ state of Γ_5(C) excitons in $CuAlSe_2$ and $CuGaSe_2$ crystals.

0.5 equals 4.6 meV, while the longitudinal–transversal splitting does not exceed 3.4 meV.

4. Conclusions

Ground and excited states of the Γ_4(A), Γ_5(B) and Γ_5(C) excitons are observed in exciton spectra of $CuAl_{1-X}Ga_XSe_2$ solid solutions. The exciton lines are situated in the energy interval from 1.74 to 2.83 eV for all compositions of the solid solution. Ground $n = 1$ and excited $n = 2$ lines of Γ_4(A), Γ_5(B) and Γ_5(C) excitons are observed in wavelength modulated reflectivity spectra of all solid solution compositions. The energy position of the $n = 1$ line of Γ_4(A), Γ_5(B) and Γ_5(C) excitons depends nonlinearly on the X value, being described by a polynomial with the coefficient of nonlinearity C equal to 0.07–0.10, which is smaller as compared to other solid solutions such as $CuGa(S_XSe_{1-X})_2$ ($C = 0.39$), $CuIn_XGa_{1-X}S_2$ ($C = 0.31$), and $CuAl_XGa_{1-X}S_2$ ($C = 0.32$). The exciton binding energy and the energy intervals $\Gamma_7(V_1)$–$\Gamma_6(C_1)$, $\Gamma_6(V_2)$–$\Gamma_6(C_1)$, $\Gamma_7(V_3)$–$\Gamma_6(C_1)$ decrease linearly with the transition from $CuGaSe_2$ to $CuAlSe_2$. The value of the damping parameter for mixed compositions is higher as compared to its value in non-mixed compositions. The damping parameter does not exceed 3 meV for compounds with $X = 1$ and 0. The effective electron mass (m^*_{c1}) decreases from $0.14m_0$ to $0.11m_0$ with transition from $CuAlSe_2$ to $CuGaSe_2$, while the effective hole mass (m^*_{V1}) decreases from $1.26m_0$ to $1.20m_0$.

The wavelength modulated reflectivity spectra allow one to determine more reliably the energy position of excited exciton states and to evaluate the asymmetry parameter of ground exciton states. The asymmetry parameter was found to be nearly the same for all compositions, and it varies in the range of 0.02–0.06, i.e. the sign of the asymmetry coefficient for the $n = 1$ line of A, B, and C excitons is positive for all compositions of the solid solutions.

References

[1] Boyd G D, Kasper H and Mc Fee J H 1971 *IEEE J. Quantum Electron.* **7** 563
[2] Wagner S, Shay J L and Kasper H M 1975 *Appl. Phys. Lett.* **27** 89

[3] Gabor A M, Tuttle J R, Albin D S, Tennant A L and Coutreras M A 1994 *AIP Conf. Proc.* **306** 59
[4] Fan Y X, Eckard R C, Byer R L, Route R K and Feigelson R S 1984 *Appl. Phys. Lett.* **45** 313
[5] Tanaka K, Uchiki H, Iida S, Terasako T and Shirakata S 2000 *Solid State Commun.* **114** 197
[6] Syrbu N N, Ursaki V V, Tiginyanu I M, Tezlevan V E and Blaje M A 2003 *J. Phys. Chem. Solids* **64** 1967
[7] Susaki M, Yamamoto N and Wakita K 2001 *Japanese Research Review and Ternary and Multinary Compounds for Pioneering the 21st Century* (*JPAP Book Series 1*) (Tokyo: Institute of Pure and Applied Physics)
[8] Syrbu N N, Blaje M, Tiginyanu I M and Tezlevan V E 2002 *Opt. Spectrosc.* **92** 395
[9] Susaki M, Wakita K, Yamamoto N, Niwa E and Masumoto K 1998 *Japan. J. Appl. Phys.* **37** 847
[10] Terasako T, Umiji H, Tonaka K, Shiratata S, Uchiki H and Jsomura S 1998 *Japan. J. Appl. Phys.* **38** 805
[11] Susaki M, Wakita K and Jamamoto N 1999 *Japan. J. Appl. Phys.* **38** 2287
[12] Syrbu N N, Blaje M, Tezlevan V E and Ursaki V V 2002 *Opt. Spectrosc.* **92** 402
[13] Shay J L and Wernick J H 1975 *Ternary Chalcopyrite Semiconductors: Growth, Electronic Properties, and Applications* (Oxford: Pergamon)
[14] Birkmire R W and Eser E 1997 *Annu. Rev. Mater. Sci.* **27** 625
[15] Ramanathan K *et al* 2003 *Prog. Photovolt.* **11** 225
[16] Chichibu S, Shirakata S, Ogawa A, Sudo R, Uchida M, Harada Y, Wakiyama T, Shishikura M, Matsumoto S and Isomura S 1994 *J. Cryst. Growth* **140** 388
[17] Bodnar I V, Rudi V Yu and Rudi Yu V 1994 *Fiz. Tekhn. Poluprovodn* **28** 1755
[18] Zaretskaya E, Gremenok V, Zalesski V, Schorr S, Rud V and Rud Yu 2009 *Phys. Status Solidi* **6** 1278
[19] Ahuya R, Auluck S, Eriksson O, Wills J M and Johansson B 1998 *Sol. Energy Mater. Sol. Cells* **53** 357
[20] Jaffe J E and Zunger A 1983 *Phys. Rev.* B **28** 5822
Jaffe J E and Zunger A 1984 *Phys. Rev.* B **29** 1882
[21] Koster G F, Dimmock J O, Wheeler R G and Statz H 1963 *Properties of Thirty-Two Point Groups* (Cambridge: Massachusetts Institute of Technology)
[22] Kawashima T, Adachi S, Miyake H and Sugiyama K 1998 *J. Appl. Phys.* **84** 5202
[23] Betini M 1973 *Solid State Commun.* **13** 599
[24] Shirakata S, Ogawa A, Isomura S and Kariya T 1993 *Japan. J. Appl. Phys.* **32** (Suppl. 32-3) 94
[25] Alonso M I, Garriga M, Durante C A, Rincon M and Leon M 2000 *J. Appl. Phys.* **88** 5796
[26] Andriesch A M, Syrbu N N, Iovu M S and Tezlevan V E 1995 *Phys. Status Solidi* b **187** 83
[27] Syrbu N N, Bogdanash M, Tezlevan V E and Stamov I G 1997 *J. Phys.: Condens. Matter* **9** 1217
[28] Syrbu N N, Bogdanash M, Tezlevan V E and Mushkutariu I 1997 *Physica* B **229** 199
[29] Pekar S I 1958 *Zh. Eksp. Teor. Fiz.* **34** 1176
[30] Agranovich V M and Ginzburg V L 1966 *Spatial Dispersion in Crystal Optics and the Theory of Excitons* (New York: Interscience–Wiley)
[31] Ivchenko E L 1982 *Exitons* ed E A Rasba and M D Struge (Amsterdam: North-Holand) p 141
[32] Selkin A 1977 *Phys. Status Solidi* b **83** 47
[33] Permogorov S A, Travnicov V V and Selkin A V 1972 *Fiz. Tverd. Tela* **14** 3642
[34] Levcenko S, Syrbu N N, Tezlevan V E, Arushanov E, Merino J M and León M 2008 *J. Phys. D: Appl. Phys.* **41** 0055403
[35] Mandel L, Tomlinson R D, Hampshire M J and Neuman H 1979 *Solid State Commun.* **32** 201
[36] Weinert H, Neuman H, Hebler H, Kun G and Nam N 1977 *Phys. Status Solidi* b **81** K59
[37] Wasim S 1983 *Phys. Status Solidi* a **75** K69
[38] Syrbu N N, Tiginyanu I M, Nemerenko L L, Ursaki V V, Tezlevan V E and Zalamai V V 2005 *J. Phys. Chem. Solids* **66** 1974
[39] Syrbu N N, Tiginyanu I M, Ursaki V V, Tezlevan V T, Zalamai V V and Nemerenko L L 2005 *Physica* B **365** 43
[40] Syrbu N N, Nemarenco L L and Tezlevan V T 2007 *Opt. Mater.* **30** 451
[41] Syrbu N N, Nemerenco L L, Stamov I G, Bejan V N and Tezlevan V T 2007 *Opt. Commun.* **272** 124
[42] Toyozawa Y 1958 *Progr. Theor. Phys.* **19** 214
Toyozawa Y 1958 *Progr. Theor. Phys.* **20** 53
Toyozawa Y 1962 *Progr. Theor. Phys.* **27** 89
[43] Hopfield J J 1958 *Phys. Rev.* **112** 1555